

Adult mouse subventricular zones stimulate glioblastoma stem cells specific invasion through CXCL12/CXCR4 signaling

Nicolas Goffart, Jérôme Kroonen, Emmanuel Di Valentin, Matthias Dedobbeleer, Alexandre Denne, Philippe Martinive, and Bernard Rogister

Laboratory of Developmental Neurobiology, GIGA-Neurosciences Research Center, University of Liège, Liège, Belgium (N.G., A.D., M.D., B.R.); Human Genetics, CHU and University of Liège, Liège, Belgium (J.K.); The T&P Bohnenn Laboratory for Neuro-Oncology, Department of Neurosurgery, University Medical Center Utrecht, Utrecht, The Netherlands (J.K.); GIGA-Viral Vector Platform, University of Liège, Liège, Belgium (E.D.V.); Unit of Radiology and Radiotherapy, CHU and University of Liège, Liège, Belgium (P.M.); Department of Neurology, CHU and University of Liège, Liège, Belgium (B.R.); GIGA-Development, Stem Cells and Regenerative Medicine, University of Liège, Liège, Belgium (B.R.)

Corresponding Author: Bernard Rogister, PhD, GIGA-Neurosciences – Development, Stem Cells and Regenerative Medicine, Université de Liège, Avenue de l'Hôpital, 1, 4000 Liège, Belgium (bernard.rogister@ulg.ac.be).

Background. Patients with glioblastoma multiforme (GBM) have an overall median survival of 15 months. This catastrophic survival rate is the consequence of systematic relapses that could arise from remaining glioblastoma stem cells (GSCs) left behind after surgery. We previously demonstrated that GSCs are able to escape the tumor mass and specifically colonize the adult subventricular zones (SVZs) after transplantation. This specific localization, away from the initial injection site, therefore represents a high-quality model of a clinical obstacle to therapy and relapses because GSCs notably retain the ability to form secondary tumors.

Method. In this work, we questioned the role of the CXCL12/CXCR4 signaling in the GSC-specific invasion of the SVZs.

Results. We demonstrated that both receptor and ligand are respectively expressed by different GBM cell populations and by the SVZ itself. In vitro migration bio-assays highlighted that human U87MG GSCs isolated from the SVZs (U87MG-SVZ) display stronger migratory abilities in response to recombinant CXCL12 and/or SVZ-conditioned medium (SVZ-CM) compared with cancer cells isolated from the tumor mass (U87MG-TM). Moreover, in vitro inhibition of the CXCR4 signaling significantly decreased the U87MG-SVZ cell migration in response to the SVZ-CM. Very interestingly, treating U87MG-xenografted mice with daily doses of AMD3100, a specific CXCR4 antagonist, prevented the specific invasion of the SVZ. Another in vivo experiment, using CXCR4-invalidated GBM cells, displayed similar results.

Conclusion. Taken together, these data demonstrate the significant role of the CXCL12/CXCR4 signaling in this original model of brain cancer invasion.

Keywords: cancer stem cells, CXCL12, invasion, stem cell microenvironment.

Primary brain tumors are among the most refractory of malignancies. Their most aggressive form, glioblastoma multiform (GBM, WHO grade IV), is also the most common and lethal subtype.¹ Although multimodal therapies have been developed, the overall median survival of GBM patients hardly reaches 15 months from the time of diagnosis.² This poor survival rate is the consequence of tumor recurrence that systematically occurs despite classical therapeutic strategies. Trying to understand the origin of GBM relapses seems mandatory, in this context, for a better understanding of the tumor's biology and improving the patients' quality of life.

The infiltrative patterns of GBM make tumor cells hard to target. Furthermore, recent studies using orthotopic xenografts have demonstrated that GBM cells are able to escape the tumor mass and specifically invade the subventricular zones (SVZs) of the adult brain.^{3,4} In that environment, GBM cells were first shown to be highly tumorigenic and were later characterized as glioblastoma stem cells (GSCs). The SVZ is known to be the major source of neural stem cells and progenitors in adults and functions as a supportive niche promoting self-renewal and inhibits differentiation.^{5,6} This "seed-and-soil" relationship has also been adapted to cancer stem cell research

Received 30 December 2013; accepted 24 June 2014

© The Author(s) 2014. Published by Oxford University Press on behalf of the Society for Neuro-Oncology. All rights reserved. For permissions, please e-mail: journals.permissions@oup.com.

because GSCs also rely on a specific environment or niche to maintain their stem cell properties and their ability to drive tumor growth.^{7,8}

In this work, we questioned the role of the CXCL12/CXCR4 signaling in the GSC-oriented invasion of the SVZ. CXCR4 is known to be expressed by highly malignant gliomas,^{9,10} be involved in tumor cell proliferation,¹¹ and be associated with a poor survival.¹² Recent studies have shown that CXCL12 and CXCR4 enhance tumorigenesis through increased proliferation of tumor cells¹³ and that CXCL12 boosts the release of vascular endothelial growth factor (VEGF) from GSC, leading to tumor growth-induced angiogenesis.¹⁴ When taken altogether, those facts led to investigating the eventual role of the CXCR4 signaling in the specific invasion of the SVZ by human GSC. Counteracting with the invasion abilities of GSC would make those cells more easily targeted by classical therapeutic strategies and would definitely improve the survival rate for GBM patients.

Materials and Methods

Cell Culture

Primary GBM cultures (GBM1, GBM2, and GB138) were established from consenting participants and validated as previously described.^{3,15} Human GBM cell lines (U87MG ATCC HTB-14, U373 [a generous gift from Florence Lefranc], and LN18 ATCC CRL-2610) were cultivated in Dulbecco's modified Eagle's medium (DMEM) containing 10% fetal bovine serum (Invitrogen). Details can be found in Supplemental Experimental Procedures.

Ethics Statement

Participants gave their informed consent for use of GBM specimens. The use of human tissue has been allowed by the "Comité d'éthique Hospitalo-Universitaire du CHU de Liège". This use concerns only residual material after surgical tumor resection.

Animals

Adult P40 female immunodeficient nude mice, Crl:NU-Foxn1^{nu}, obtained from Charles River Laboratories, were used for xenografts and ventricular surface studies. All animals were cared for in accordance with the Declaration of Helsinki and following the guidelines of the Belgium Ministry of Agriculture in agreement with European Commission Laboratory Animal Care and Use Regulation (86/609/CEE, CE of J n_L358, 18 December 1986). The athymic nude mice were housed in sterilized, filter-topped cages and were processed as approved by the Animal Ethical Committee of the University of Liège.

Whole Mount Dissection

The lateral walls of the ventricles were dissected from the caudal aspect of the telencephalon, as previously described.¹⁶ Detailed procedures can be found in Supplemental Experimental Procedures.

Intracranial Transplantation

Intracranial xenografts were generated, as described previously.³ Detailed procedures can be found in Supplemental Experimental Procedures.

In Vitro Migration Bio-assays

Chemotaxis assays were performed using a 96-well chemotaxis chamber with 10 μ m pore size (NeuroProbe). GBM cell lines were labeled using a Cell Tracker Green (CTG) dye (Invitrogen) at a final concentration of 5 μ M in prewarmed DMEM for 30 minutes. The medium was replaced with DMEM and incubated for 30 minutes at 37°C. Cells were washed 3 times with phosphate-buffered saline (PBS) and seeded in the upper chamber (25 000 cells in 25 μ l of serum-free medium without growth factors). The lower chamber was filled with 28 μ l of serum-free medium, SVZ-conditioned medium, SVZ-conditioned medium containing AMD3100 (25 μ g/ml, Sigma), or serum-free medium with different concentrations of human recombinant CXCL12 (Peprotech). After incubation at 37°C for 16 hours, cells in the lower chambers were fixed with 4% paraformaldehyde (PFA) for 15 minutes. Chambers were rinsed, and the total number of migrating cells was quantified by counting the number of CTG-positive cells per well ($n = 3$) for each condition.

Time-lapse Analysis

Live chemotaxis was measured by means of μ -Slides (Ibidi GmbH) according to the manufacturer's instructions.¹⁷ Detailed procedures can be found in Supplemental Experimental Procedures.

Western Blot Analysis

Protein extracts were resolved with Novex 10% Bis-Tris gels (NuPAGE, Invitrogen) and transferred onto a PVDF membrane (Roche) according to standard protocols. Blots were then probed with primary and secondary antibodies. Blots were imaged with the ImageQuant 350 scanning system (cooled-CCD camera, GE Healthcare). Detailed procedures and buffer composition can be found in Supplemental Experimental Procedures.

Gene Expression Profiling Using Real-time PCR Arrays

SVZs were dissected as previously described ($n = 12$), and total RNA was isolated using Trizol reagent (Invitrogen) and then re-purified using a column (RNeasy Mini Kit; Qiagen) according to the manufacturer's protocol. PCR array analysis was performed using RT² profiler PCR array (mouse chemokines and cytokines, PAMM-150, SABiosciences). Detailed procedures can be found in Supplemental Experimental Procedures.

Real-time PCR

Total RNA was isolated using the RNeasy Mini Kit (Qiagen) according to the manufacturer's protocol. Detailed procedures can be found in Supplemental Experimental Procedures.

Processing of Tissue Sections and Cell Cultures Before Immunostaining

Mice were anesthetized with an injection of Nembutal (pentobarbital 60 mg/mL, Ceva Sante Animal) before an intracardiac perfusion with a NaCl 0.9% solution (Prolabo, VWR International) followed by 4% PFA at 4°C (4,3 g/L NaOH, 40 g/L paraformaldehyde, 18.8 g/L NaH₂PO₄). Brains were collected, postfixed in 4% PFA, and cryoprotected overnight in a solution of PBS/sucrose (20%). Brains were frozen at -20°C in a 2-methylbutane solution (Sigma) and cut into 16 µm thick coronal sections using a cryostat. For immunocytofluorescence, cells were placed on coverslips previously coated with polyornithine for 3 hours (0.1 mg/mL, Sigma). Cells were washed in PBS, fixed in 4% PFA for 15 minutes, and washed in PBS.

Immunostaining

Brain coronal sections or GBM cells were permeabilized, and un-specific binding sites were blocked using 10% donkey serum and 0.1% Triton X-100 PBS solution. Tissue sections or cells were incubated with primary antibodies diluted in PBS containing 0.1% donkey serum and 0.1% Triton X-100, followed by a second incubation with RRX- or FITC-conjugated secondary antibodies (1:500, Jackson ImmunoResearch Laboratories). Detailed procedures can be found in Supplemental Experimental Procedures.

Enzyme-linked Immunosorbent Assay Analysis

CXCL12 concentrations in SVZ/cerebellum/olfactory bulb (OB)-conditioned medium were analyzed by sandwich enzyme-linked immunosorbent assay (ELISA) according to the manufacturer's instructions (R&D Systems).

Plasmids, Lentiviral Vectors Generation, and Transduction

Detailed information and procedures can be found in Supplemental Experimental Procedures.

Bioluminescence Imaging

Immunodeficient nude mice bearing intracranial xenografts were injected intraperitoneally with D-luciferin (150 mg/kg, Sigma). After anesthesia using 2.5% isoflurane, mice were imaged with a charge-coupled device camera-based bioluminescence imaging system (IVIS 50, Xenogen; exposure time 1–30 s, binning 8, field of view 12, f/stop 1, open filter). Signals were displayed as photons/s/cm²/sr. Regions of interest were defined manually, and images were processed using Living Image and IgorPro Software (Version 2.50). Raw data were expressed as total photon flux (photons/s).

Image Acquisition and Data Analysis

Immunostained sections were imaged using a laser-scanning confocal microscope equipped with a krypton/argon gas layer (Olympus Fluoview 1000). Zeiss Axiovert 10VR microscope (Carl Zeiss), coupled with Mercator software (Explora Nova),

was used for cell counting and 3D reconstructions. Figures were composed and examined using ImageJ.

Statistical Analysis

Quantitative data are expressed as mean ± SEM. Two-way ANOVA, followed by a Tukey posttest was used, and a *P* value <0.05 was considered statistically significant. Student *t* tests were performed for 2 groups were compared using Statistica 10.0 software.

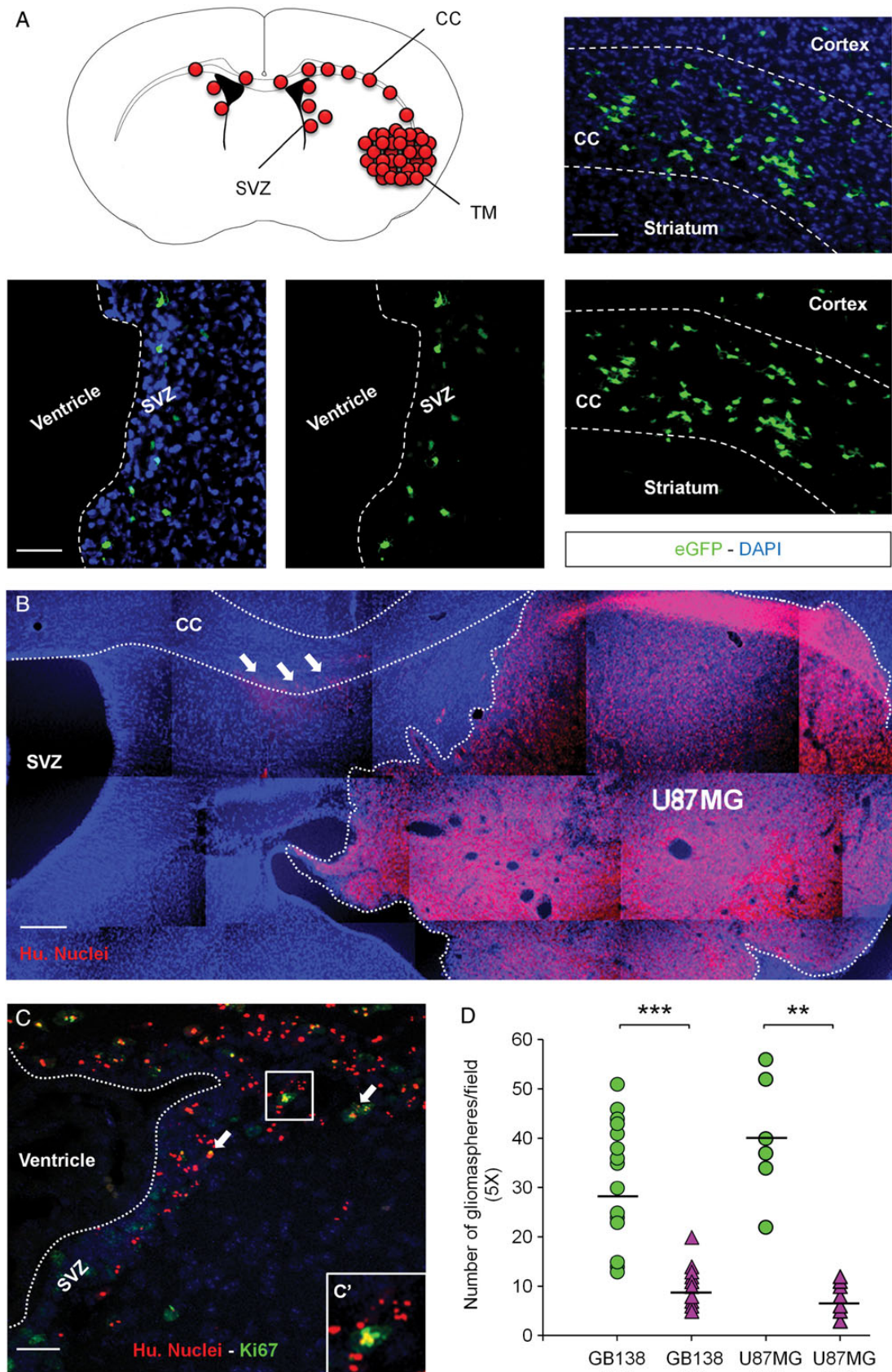
Results

In Vivo Model of GSC Invasion

We previously demonstrated that human GSCs are able to invade the SVZ environment once injected in the striatum of immunodeficient mice.³ Using this model of cancer cell invasion, we grafted human primary GBM cells (GB138) expressing eGFP in the striatum of mice tolerating xenografts. Twelve weeks after the injection, as the mice developed tumors (TM), we identified primary GB138 cells in the SVZ environment. As expected, those cells migrated along the corpus callosum (CC), one of the main white matter structures connecting both left and right hemispheres together (Fig. 1A). We then validated this specific model of SVZ invasion with human U87MG cells, which were injected into the striatum of immunodeficient mice as well. Three weeks after the injections, we identified U87MG cells in the CC of mice using specific antihuman nuclei antibodies (white arrows, Fig. 1B). By the end of the fourth week after the graft, human U87MG cells had colonized the SVZ environment, with some of the cells retaining their ability to proliferate as shown by a Ki67-positive staining (white arrows, Fig. 1C and C'). Relying on this specific model of brain cancer invasion, we isolated U87MG and GB138 cells from the TM (U87MG-TM and GB138-TM) and from the SVZs (U87MG-SVZ and GB138-SVZ). We tested the ability of those 4 cell subtypes to form gliomaspheres (Fig. 1D). Being able to form gliomaspheres is indeed part of the cancer stem cell definition.¹⁸ Interestingly, both U87MG-SVZ and GB138-SVZ cells were better to grow as floating spheres compared with U87MG-TM cells (*P* = .002) and GB138-TM cells (*P* = .0001).

Expression of Chemokines in the SVZ Environment

In order to identify potential targets involved in the GSC-specific invasion of the SVZ, we looked for soluble factors secreted by the SVZ environment that could eventually play a role in this migration phenotype. To do so, total mRNA extractions from 12 independent SVZ whole mounts were performed, and a wide scale RT-qPCR array was conducted. This analysis highlighted high mRNA levels (*Ccl12*, *Ccl19*, *Cxcl12* and *Cx3cl1* - [yellow rim of the graph]), basal mRNA levels (*Ccl5*, *Ccl17*, *Cxcl10* and *Cxcl16* [purple rim of the graph]), and low mRNA levels (*Xcl1*, *Ccl1*, *Cxcl3* and *Cxcl9* [white rim of the graph]) of cytokines and chemokines present in the SVZ environment (Fig. 2A). This database provides a “big picture” summary of the different factors that could be involved in the GSC-specific invasion of the SVZ. From those data, we identified CXCL12 as the main target of our study. Indeed, CXCL12 has already been shown to be



involved in glioma cell proliferation.^{19,20} We first confirmed CXCL12 mRNA expression on SVZ whole mounts, using mesenchymal stem cells as a positive control (Fig. 2B). We studied the expression of CXCL12 on brain coronal sections of mice previously injected with human U87MG cells and highlighted a close relationship between the expression of CXCL12 and the presence of U87MG GSC in the SVZ (Fig. 2C). We confirmed that observation on coronal sections of brains injected with human GB138 primary cells labeled with eGFP (Fig. 2D and E). We managed to put to light a gradient of CXCL12 within the SVZ environment (Fig. 2F). To do so, we transformed each CXCL12 acquisition from the SVZ environment into binary images and quantified the CXCL12 expression in predefined areas (A, SVZ; B, transition SVZ-striatum; C, striatum). We systematically found a constant decrease of the CXCL12 expression starting from area A to C. This suggests that CXCL12 is mostly secreted in the SVZ and diffuses towards the striatum along a decreasing concentration gradient. To further explore the expression of CXCL12, we decided to compare, by ELISA, the secretion of CXCL12 within the SVZ with other regions of the brain such as the cerebellum and the OBs. We found a significant increase of the CXCL12 expression within the medium conditioned by SVZ whole mounts for 60 hours compared with 24 hours ($P = .0006$). Moreover, a significantly higher amount of CXCL12 was found in the medium conditioned by SVZ whole mounts for 60 hours compared with media conditioned either by OB or cerebellum whole mounts for 60 hours ($P = .005$) (Fig. 2G). This shows how specific the CXCL12 expression is to the SVZ region. We finally demonstrated that the blood vessels overlaying the lateral wall of the ventricle (lectin staining) and the astrocytes (glial fibrillary acid protein [GFAP] staining) were sources of CXCL12 in the adult brain (Fig. 2H).

Expression of CXCR4 by Human GBM Cells

We then tackled the expression of CXCL12 receptors on human GBM cells. Using reverse transcription (RT)-PCR and Western blot approaches, we highlighted the expression of CXCR4 on 3 GBM cell lines (U87MG, U373, and LN18) and 2 GBM cell populations in primary cultures (GBM1 and GBM2) (Fig. 3A and B). We also checked the CXCR4 expression profile on U87MG cells, U87MG cells isolated from the TM (U87MG-TM), U87MG cells from the SVZ (U87MG-SVZ), and U87MG cells cultured as floating spheres (U87MG NS). We noticed a comparable expression of CXCR4 in each of these cell populations (Fig. 3C). We then characterized the U87MG spheres for the expression of CXCR4, together with immature markers and differentiation markers. Immunostained spheres revealed that CXCR4 is mainly associated with proteins such as Nestin, Sox2, β III-Tubulin, and GFAP on GBM cells (Fig. 3D). We finally characterized gliomaspheres from U87MG-TM and U87MG-SVZ cells and labeled them with different GSC markers such as Prolamin-1 (CD133) or Integrin α 6 (ITGA6).²¹ We demonstrated here that both gliomasphere subpopulations expressed important levels of CXCR4, Nestin, CD133, and ITGA6 (Fig. 3E).

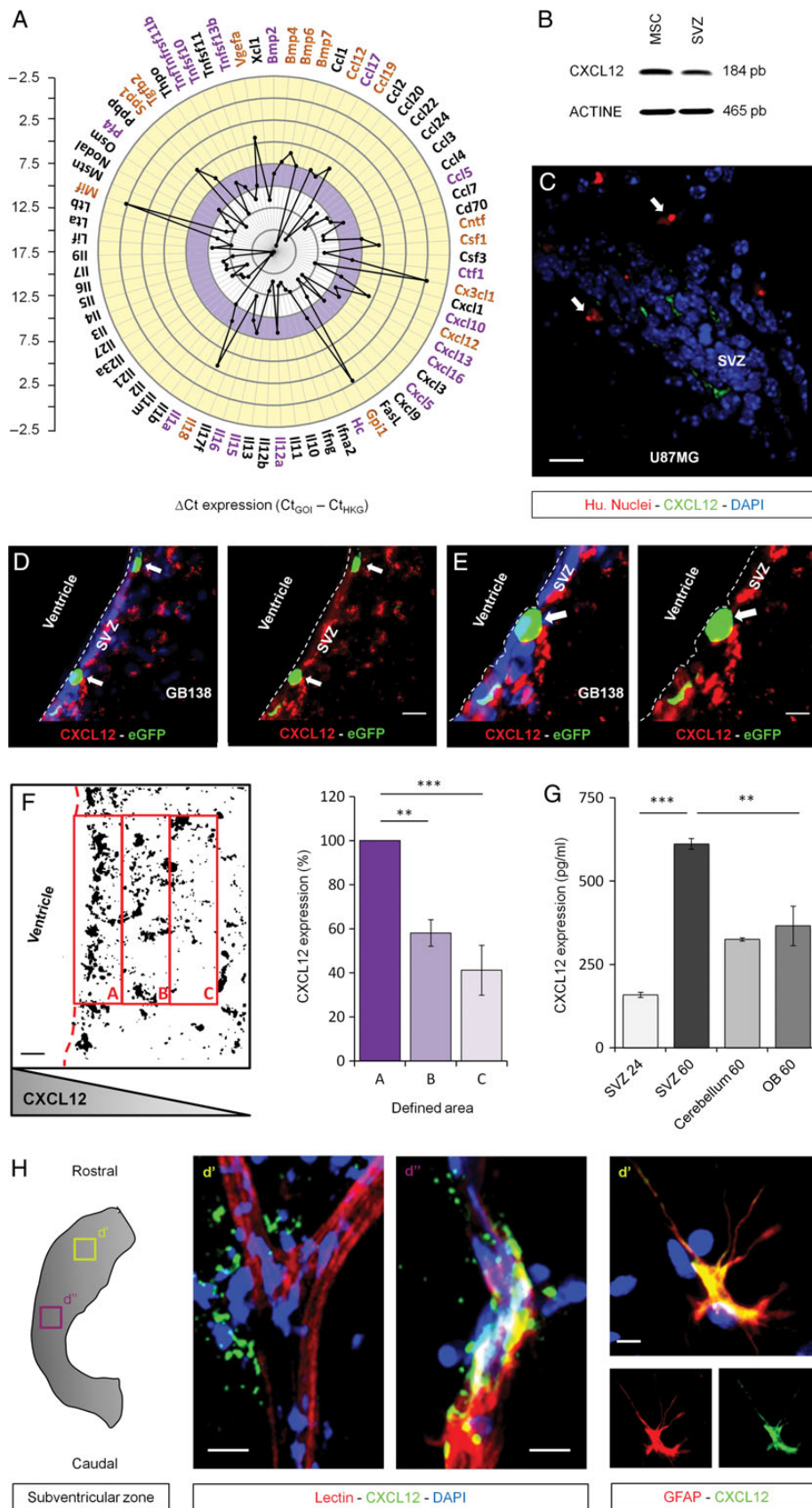
We know that CXCL12 can bind a second chemokine receptor, CXCR7.²² This recently discovered receptor is the center of attention in many publications on GBM, but its role in tumorigenesis remains unclear.^{23,24} As far as we are concerned, we have not been able to detect a convincing CXCR7 expression by immunohistofluorescence or Western blot analyses (data not shown), making it unlikely to be involved in our model.

AMD3100 Disrupts Chemotactic Effects of SVZ-conditioned Medium on GBM Cells

To investigate whether human GBM cells home to the SVZ through secreted factors in a direct manner, we brought a modified Boyden chamber assay into focus. Human GBM cells were suspended in serum-free medium and seeded on top of a porous membrane, separating them from a bottom chamber filled with test or control media, which allowed the cells to move into the bottom part of the chamber in response to the chemotactic agent of interest. We first tested the ability of U87MG cells to migrate in response to various concentrations of CXCL12 and serial dilutions of SVZ-CM. U87MG cells displayed a dose-dependent migration behavior in response to both stimulations (Fig. 4A and C). To confirm the U87MG tropism towards a gradient of CXCL12 and SVZ-CM, we seeded U87MG cells in chemotaxis μ -Slides. We then recorded and analyzed the U87MG cell tracks over a period of 20 hours in response to both stimulations. The overall distribution of migration angles was analyzed and revealed significant clusters of migration direction in response to the CXCL12 gradient ($P < .001$) (Fig. 4B) and the SVZ-CM gradient ($P = .0006$) (Fig. 4D).

We then evaluated the impact of AMD3100 on the U87MG cell migration using our modified Boyden chamber assays. CXCL12/CXCR4 signaling can indeed be blocked using AMD3100,²⁵ a bicyclam noncompetitive antagonist of CXCR4.²⁶ Adding AMD3100 (25 nM) in the SVZ-CM was followed by a significant reduction (-28.2%) of the number of U87MG cells ($P = .005$) migrating through the filter. AMD3100 also inhibited the migration abilities of GBM primary cells in response to the SVZ-CM (-38.6% , GBM2; $P = .0001$) (Fig. 4E). The impact of AMD3100 was once again confirmed on U87MG cells using cell-track recordings and time-lapse analyses. AMD3100 clearly disrupted the U87MG distribution of migration angles in response to SVZ-CM ($P = .697$) (Fig. 4F) compared with SVZ-CM alone (Fig. 4D). However, AMD3100 did not impact the mean accumulated distance or velocity of U87MG cells, suggesting that other chemokines in the SVZ-CM could

Fig. 1. Invasion of the subventricular zone (SVZ) by U87MG cells and GB138 primary cells after intrastriatal implantation. (A) Human GB138 cells specifically colonized the SVZ environment after migration through the corpus callosum (CC). (B) Human U87MG cells invaded the largest part of the right striatum 3 weeks after the graft. At this point, U87MG cells had already escaped the tumor mass (TM) and began to migrate along the CC (white arrows). (C) U87MG cells finally invaded the SVZ environment 4 weeks after the injection, with some of them still being in a proliferation state (white arrows, magnified square). (D) U87MG and GB138 cells isolated from the SVZ displayed stronger abilities to form gliomaspheres than U87MG or GB138 cells isolated from the TM. Human U87MG cells were detected using an antihuman nuclei antibody (Hu. Nuclei - red). GB138 cells were engineered to express the green fluorescent protein (eGFP - green). Cell nuclei were counterstained with DAPI (blue). Scale bars = 500 μ m for B, 40 μ m for A and C. ** $P < .01$, *** $P < .001$.



also play a role in the in vitro U87MG migration behavior in response to SVZ-CM (Fig. 4G and H).

We finally compared how U87MG cells, U87MG-TM cells (isolated from the tumor mass), and U87MG-SVZ cells (isolated from the SVZ) behaved in response to recombinant CXCL12 or SVZ-CM supplemented or not with AMD3100. Surprisingly, U87MG-SVZ cells displayed greater migration ability in response to recombinant CXCL12 than U87MG cells or U87MG-TM cells ($P < .0001$). Similarly, U87MG-SVZ cells were also more attracted by the SVZ-CM in comparison with the other cell populations ($P < .0001$). Interestingly, the in vitro inhibition of migration by AMD3100 was also more obvious on the U87MG-SVZ cell population compared with their counterparts isolated from the tumor mass. Using AMD3100 (25 nM) allowed to decrease the U87MG-TM and U87MG-SVZ migration levels up to 17.7% (not statistically significant) and 44.2% respectively ($P < .0001$) (Fig. 4I), suggesting a stronger impact of the drug on GBM cells isolated from the SVZ and previously characterized as a population enriched in GSC abilities.³

Depletion of CXCR4 Inhibits the GSC Invasion of the SVZ

We generated stable CXCR4-invalidated U87MG cells using 2 different shRNA-mediated knockdowns. Those cells were also engineered to express a fusion protein of firefly luciferase and eGFP (U87MG-EIL-shCXCR4* and U87MG-EIL-shCXCR4**). Control cells for this experiment were built through expression of a scrambled shRNA (U87MG-EIL-sc).

We first confirmed the depletion of CXCR4 by Western blot analysis and validated those data by immunocytofluorescence (Fig. 5A and B). The expression of CXCR4 was downregulated by 41% and 64%, respectively, in the U87MG-EIL-shCXCR4* and U87MG-EIL-shCXCR4** cell populations (Fig. 5A). We then tested the functionality of those 2 CXCR4-depleted cell populations using modified Boyden chambers to evaluate chemotaxis in response to recombinant CXCL12. The migration of both CXCR4-depleted U87MG cells was significantly reduced, regardless of the remaining level of CXCR4 (Fig. 5C). We finally grafted the 2 populations of CXCR4-depleted U87MG cells and U87MG control cells into the striatum of immunodeficient mice. As expected, human U87MG cells, labeled with eGFP, were found in the CC and the SVZ region of control mice after 4 weeks (Fig. 5D). Surprisingly, this invasion phenotype was totally hampered in the CXCR4 knockdown conditions, in which no eGFP signal could be detected in the SVZ environment (Fig. 5E). There were no differences observed in mean body mass between groups (data not shown).

AMD3100 Inhibits the Specific GSC Invasion of the SVZ

We injected luciferase-expressing U87MG cells into the right striatum of immunodeficient nude mice. Animals bearing xenografts were separated into 2 homogeneous groups at day 25 post injection according to in vivo bioluminescence data. Indeed, U87MG cells expressing the luciferase enzyme allowed to monitor noninvasive imaging of tumor-associated bioluminescence and quantification of tumor growth over time.²⁷ Half of the cohort was treated twice a day with intraperitoneal injections of AMD3100 at a concentration of 1.25 mg/kg, whereas the other half of the cohort was treated with PBS (control). The treatment started at day 25 in order to minimize the already-known impact of AMD3100 on tumor growth¹¹ and, more specifically, to treat the mice during the particular window of time when human GSC started to invade the SVZ.³ Growth curves established from serial measurements of bioluminescence revealed a significant antitumor effect of AMD3100 in U87MG-xenografted mice ($P < .01$) (Fig. 6A). This observation was consistent with the fact that tumor volumes were on average 28% smaller in the AMD3100-treated group after histological examinations (data not shown). This reduction of tumor volume was nevertheless not statistically significant due to the high variability between animals bearing xenografts ($P = .65$).

Regarding the invasive abilities of U87MG cells, the number of GBM cells in the CC of AMD3100-treated animals was significantly reduced compared with control animals ($P < .001$) (Fig. 6B and C). More importantly, we were not able to detect the presence of any U87MG cells in the SVZ environment of AMD3100-treated animals ($P < .01$) (Fig. 6B and C). We then showed that AMD3100 does not induce U87MG cell death in xenografted animals after treatment (Supplementary data, Fig. S2). In this way, we demonstrated that the inhibition of SVZ invasion by U87MG GSC is CXCR4 dependent and not a consequence of a loss of cell viability. On the other hand, U87MG cells had left the tumor mass and specifically invaded the SVZ environment through the CC in the control animals (Fig. 6C).

Discussion

The hypothesis of cancer stem cells has often been proposed to explain therapeutic failure and recurrence in a variety of cancers including GBM.²⁸ In this case, it has been suggested that GSCs are both radioresistant^{29,30} and chemoresistant.³¹ Previously, we demonstrated that one of the known

Fig. 2. Expression of CXCL12 by the subventricular zone (SVZ) environment. (A) RT-qPCR screening notably displayed a high expression level of CXCL12 in the SVZ environment (yellow rim of the graph). (B) This observation was validated by RT-PCR using mesenchymal stem cells (MSC) as a positive control. (C–E) The expression of CXCL12 was next demonstrated on brain coronal sections. This expression was consistent with the presence of U87MG cells (Hu. Nuclei) or GB138 primary cells (eGFP) in the SVZ (white arrows). (F) CXCL12 acquisitions were processed as binary images. The mean intensity, with foreground 255 and background 0, in predefined areas of the SVZ environment (A, B, and C) was calculated. A constant decrease of the CXCL12 expression was observed starting from area A to end at area C, suggesting that CXCL12 is secreted along a decreasing concentration gradient. (G) CXCL12 levels were evaluated by ELISA in conditioned media from SVZ, cerebellum, and olfactory bulb (OB) whole mounts for 24 or 60 hours. (H) CXCL12 was expressed by astrocytes and endothelial cells within the adult SVZ. Immunostaining on organotypic whole mounts showed a closely related expression of CXCL12 (green) with the vasculature and astrocytes (red). SVZ blood vessels and astrocytes were respectively stained using a FITC-coupled lectin or a specific anti-GFAP antibody (red). Cell nuclei were counterstained with DAPI (blue). Scale bars = 20 μm for C and D and 10 μm for E and H. Caption indicates where pictures and materials were taken.

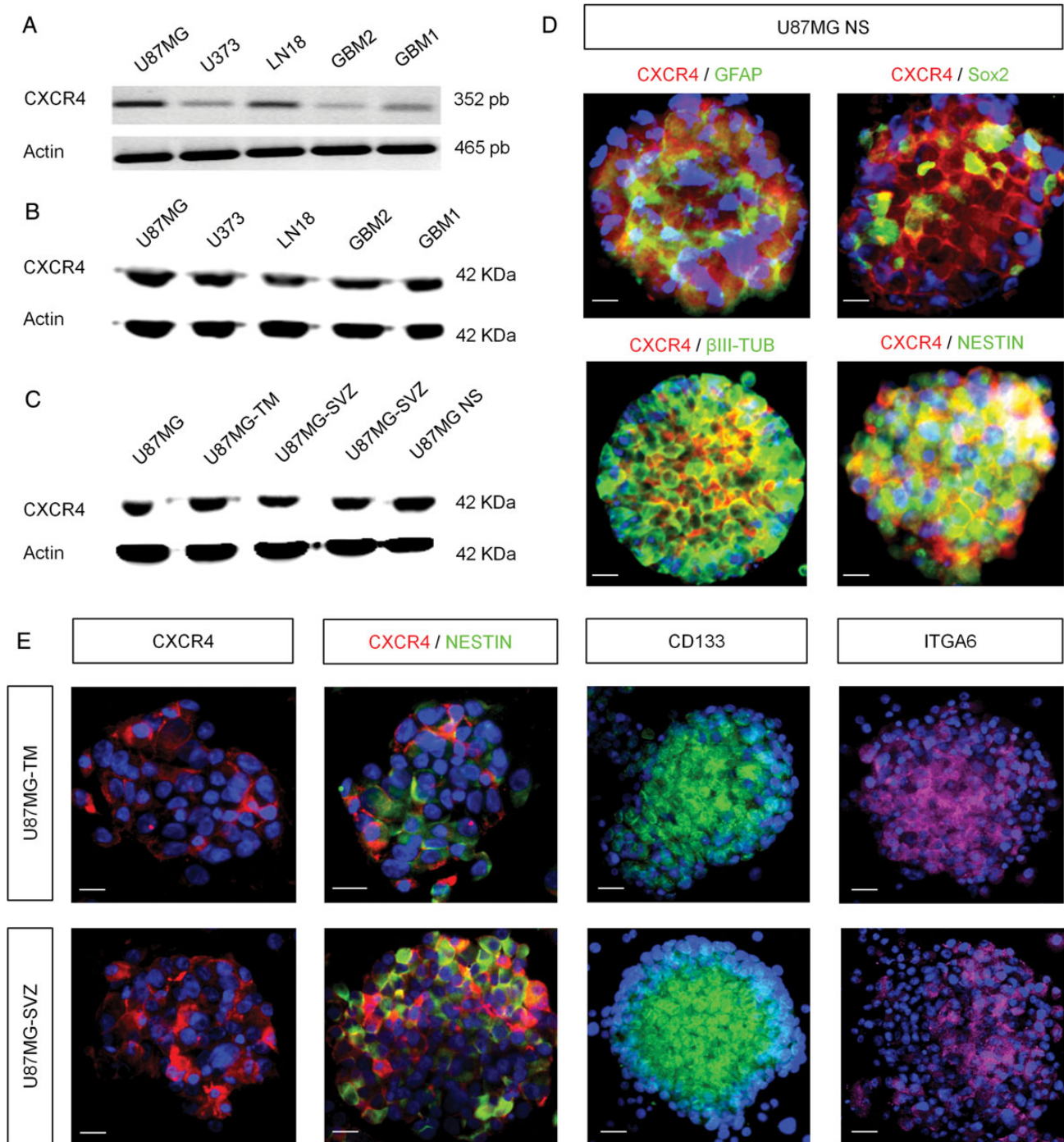


Fig. 3. Expression of CXCR4 by various GBM cell types. (A) CXCR4 mRNA expression was found in 3 human GBM cell lines (U87MG, U373, and LN18) and 2 human primary cultures (GBM 1 and 2). (B and C) Western blot analyses displayed a strong CXCR4 expression pattern in GBM cell lines and primary cultures as well as in U87MG cells isolated from the tumor mass (U87MG-TM) or the SVZ (U87MG-SVZ) and U87MG floating gliomaspheres (U87MG NS). (D) Human U87MG NS showed a combined expression of CXCR4 (red) with GFAP, Sox2, Nestin, and β III-tubulin proteins (green). (E) U87MG-TM and U87MG-SVZ gliomaspheres specifically expressed CXCR4 (red) as well as GSC markers such as CD133 (green), Nestin (green), and Integrin $\alpha 6$ (ITGA6) (pink). Nuclei were counterstained with DAPI (blue). Scale bars = 15 μ m for D and E.

neurogenic zones of the adult brain, the SVZ, was able to specifically attract and host GSCs.³ We correlated this observation with the fact that cancer stem cells often tend to hide in very

specific niches, which could help maintain their stem-like abilities and capacity to drive tumor growth^{7,8} as well as influence their intrinsic resistance to treatments.³² Moreover, this

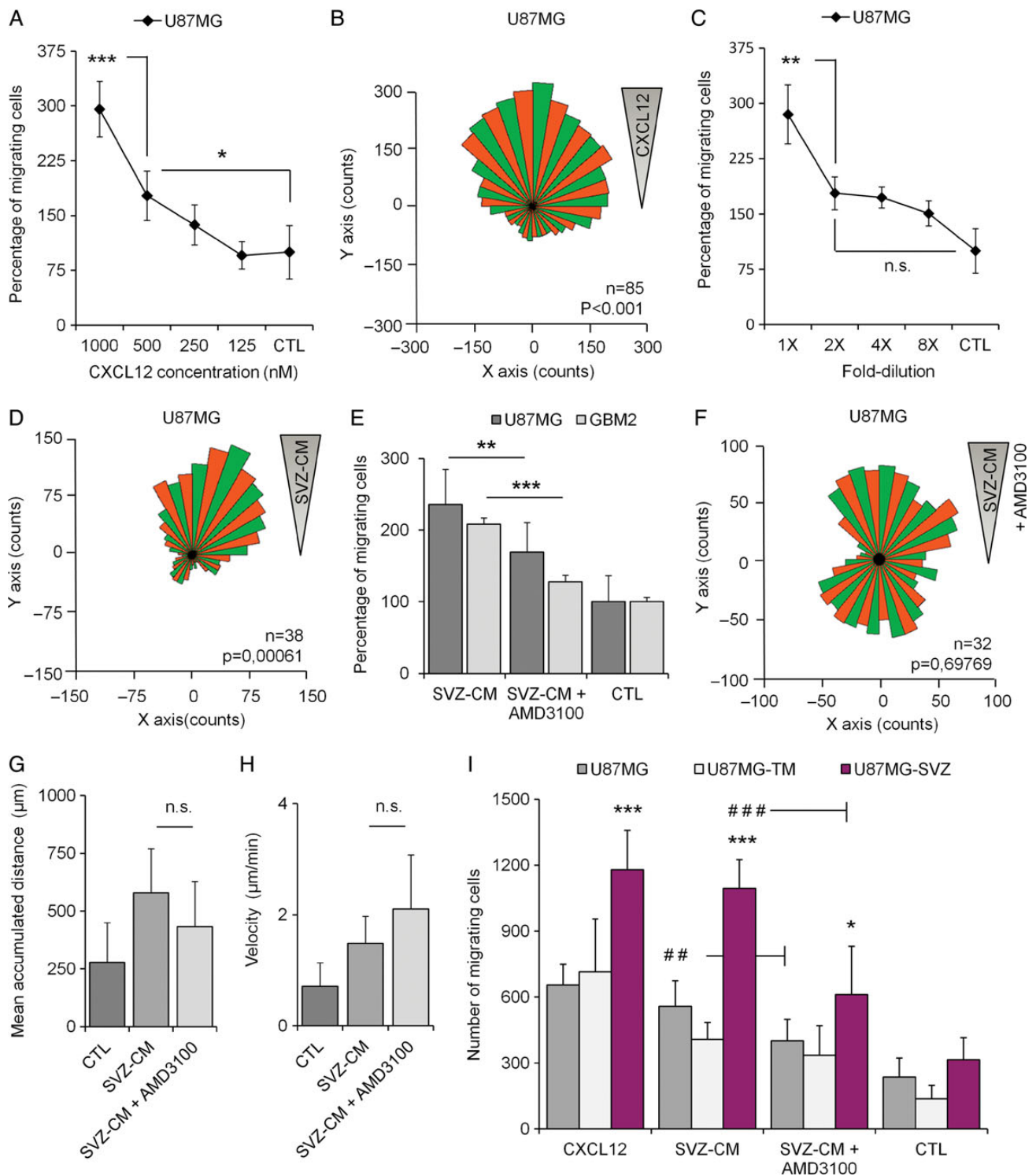


Fig. 4. In vitro migration of GBM cells in response to recombinant CXCL12 and subventricular zone-conditioned medium (SVZ-CM). (A and B) Recombinant CXCL12 triggered migration and chemotaxis of human U87MG cells. (C and D) SVZ-CM triggered migration and chemotaxis of human U87MG cells. (E) The migration of U87MG cells and human GBM cells in primary culture (GBM2) in response to SVZ-CM was significantly reduced by using AMD3100, a specific CXCR4 antagonist. (F) AMD3100 disrupted chemotaxis of U87MG cells in response to SVZ-CM. (G and H) AMD3100 did not impact parameters such as the mean accumulated distance (μm) and velocity ($\mu\text{m}/\text{min}$) of U87MG cells. (I) U87MG-SVZ cells showed greater migration abilities in response to recombinant CXCL12 and SVZ-CM compared with U87MG cells or U87MG-TM cells. Moreover, AMD3100 clearly inhibited the migration of U87MG-SVZ cells in response to SVZ-CM. Graphs are mean values \pm SEM and are representative of 3 independent experiments. * $P < .05$; ** $P < .01$; *** $P < .001$; ns, not significant.

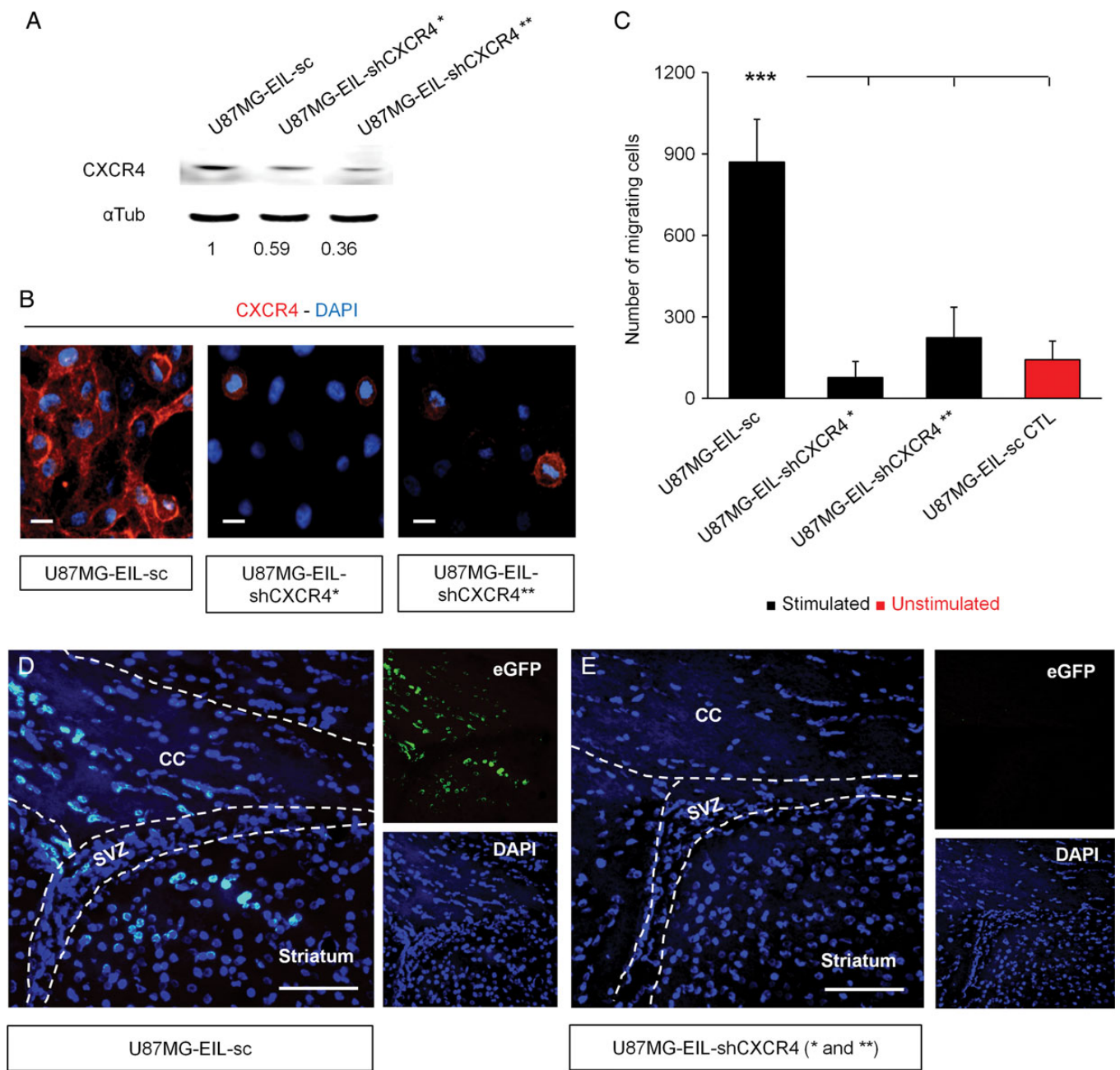


Fig. 5. Inhibition of the SVZ invasion by CXCR4-depleted U87MG cells. (A and B) Western blot and cytological analyses of the CXCR4 expression in U87MG-eGFP-Ires-Luc cells infected with lentiviruses encoding either a scrambled shRNA (U87MG-EIL-sc) or 2 short hairpins-RNA directed against CXCR4 (U87MG-EIL-shCXCR4* and U87MG-EIL-shCXCR4**). CXCR4 expression was declined up to 41% in the U87MG-EIL-shCXCR4* cells and up to 64% in the U87MG-EIL-shCXCR4** cells. (C) CXCR4 knockdown also decreased the U87MG cells in vitro migration in response to recombinant CXCL12 (1000nM) compared with the absence of CXCL12 (U87MG-EIL-sc CTL). (D and E) Animals were injected with either control U87MG cells (U87MG-EIL-sc, $n = 5$ mice) or with CXCR4-depleted U87MG cells (U87MG-EIL-shCXCR4* and U87MG-EIL-shCXCR4**, $n = 5$ mice per group). Human U87MG cells invaded the corpus callosum (CC) and the SVZ of mice grafted with U87MG-EIL-sc. No eGFP signal could be detected in the CC or the SVZ of both shRNA conditions. Scale bars = 10 μ m and 100 μ m, respectively, for B and D-E. *** $P < .001$.

observation creates an interesting parallel between GSCs and neural stem cells, which also remain located in specific neurogenic zones in order to maintain their stem cell properties.³³ A recent clinical study strengthened the link between neurogenic niches and malignant gliomas even more. This study

demonstrated that patients whose bilateral SVZs received greater than the median SVZ radiation dose showed significant improvement in progression-free survival.³⁴ Taken together, these data suggest that the SVZ environment could generously host and protect GSCs from radiation and

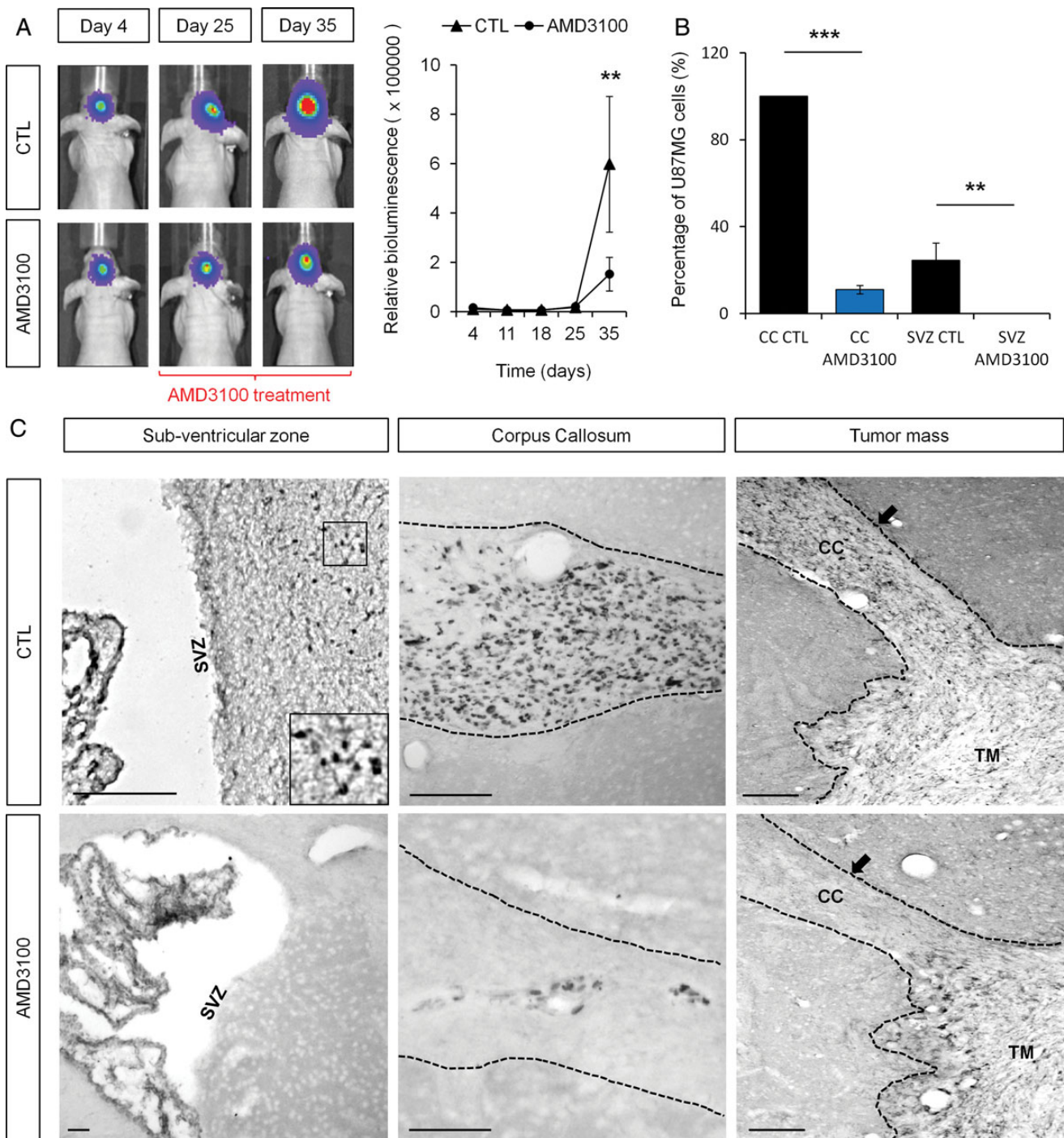


Fig. 6. AMD3100 inhibited the U87MG GSC invasion of the subventricular zone (SVZ). (A) AMD3100-treated animals showed significantly smaller amounts of relative bioluminescence compared with the control group ($P < .01$) at the end of the treatment period. (B and C) Only a few U87MG cells were found in the corpus callosum (CC) of AMD3100 treated-mice, whereas U87MG cells fully invaded the CC of PBS-treated mice (control). U87MG cells could not be found in the SVZ area in AMD3100-treated animals, whereas U87MG cells from the control group invaded the SVZ as expected. U87MG cells are labeled with a specific antihuman nuclei antibody. Scale bar = 100 μm for C. Graphs are mean values \pm SEM. ** $P < .01$, *** $P < .001$.

chemotherapy and therefore play a key role in GBM relapses.^{35,36} We should also keep in mind that the cell of origin for GBM, whether it derives from neural stem cells located in

the SVZ or another cell type, remains undefined to date.³⁷⁻³⁹ In this context, we decided to decipher the molecular mechanisms that underlie the oriented migration of GSCs to the

SVZ. Indeed, prospective identification and targeting of GSCs seem mandatory to fully understand their biology, to counteract GBM relapses, and to develop new powerful therapeutic strategies.

As a starting point, we hypothesized that chemokine receptor CXCR4 would play a role. It is known that CXCR4 is expressed by different types of cancer cells.⁹ This receptor is notably involved in cancer cell proliferation and invasiveness.^{11,40} The expression level of CXCR4 is usually associated with a poor prognosis in GBM patients¹² and has been shown to be a key mediator in GBM invasion.¹⁰ Recent findings showed that inhibition of the CXCL12/CXCR4 autocrine/paracrine loop reduces viability of human glioblastoma stem-like cells affecting self-renewal activity.⁴¹ In this work, SVZ whole mounts showed a staining pattern consistent with the expression of CXCL12 by adult SVZ blood vessels and released in the nearby environment. Interestingly, it has also been suggested that GSCs are maintained in vascular niches.⁴² We observed that the expression of CXCL12 in the SVZ is closely related to capillaries which, in turn, have been shown to play a crucial role in maintaining neural stem cell stemness in the adult brain.^{43,44} It could be tempting to hypothesize that those capillaries are also active on GSCs, notably by secreting CXCL12. In the same line, it has recently been demonstrated that brain endothelial cells secrete factors that are thought to support the expansion of GSCs by recruiting the mTOR pathway.⁴⁵ It would therefore be interesting to examine the role of the mTOR pathway in GSC invasion as a future perspective.

Human U87MG cells and GBM primary culture cells display in vitro migration abilities in response to the SVZ soluble environment (SVZ-CM). This phenotype was shown to be partially inhibited using AMD3100, a CXCR4-specific inhibitor. That observation clearly suggested the eventual role played by other chemokines in the SVZ-CM. Indeed, different mRNA levels of chemokines were detected in the SVZ environment. Several of those chemokines were found in the SVZ-CM as well. A proteome profiler analysis showed that CXCL1 was the most highly expressed chemokine in the SVZ-CM (Supplementary data, Fig. S1). This new target could be really helpful for better characterizing the controversial cell type responsible for the onset of gliomagenesis. CXCL1 has indeed been shown to promote proliferation of early oligodendrocyte progenitor cells,⁴⁶ which in turn have recently been suggested to be at the origin of malignant brain tumors.⁴⁷ Consequently, it would be worthwhile to investigate the status of CXCL1 as a target that might either support the CXCL12/CXCR4-dependent migration of GSC to the SVZ or play another role in GBM biology.

We also think it is mandatory to direct major attention to the cancer cell population isolated from the SVZ. Those cells, located away from the initial tumor mass, retain their ability to initiate development of new tumors when secondarily injected into new animals and could therefore be at the origin of GBM relapse.³ In-depth investigation on this cell subtype could provide tremendous new insights on the biology of cancer stem cells. In vitro migration bio-assays showed that U87MG cells isolated from the SVZ display enhanced migration abilities in response to CXCL12 and SVZ-CM compared with U87MG cells isolated from the tumor mass. Future analysis of the molecular response to both stimulations in these 2 different cell subtypes

thus makes sense for a better understanding of the molecular mechanisms that could lead GBM to systematically relapse and to improve current treatments.

“Inhibition of the in vivo CXCL12/CXCR4 signaling, using either lentiviral vectors allowing the expression of specific CXCR4 shRNAs or blocking CXCR4 with a specific antagonist (AMD3100) led to the same observation: GSCs were not able to home to the SVZ anymore.” Tumor volumes in the AMD3100-treated animals were on average 28% smaller than tumors in the control group but most importantly as the main message of the present work, AMD3100 partially blocked the CC invasion and prevented U87MG cells to reach the SVZ environment. From a clinical aspect, the safety of AMD3100 (also known as Plerixafor or Mozobil) has been evaluated in clinical trials²⁵ and has raised great hope for new potential clinical implications. This FDA-approved drug has successfully been tested in patients with non-Hodgkin's lymphoma and multiple myeloma, in order to support optimal stem cell mobilization for autologous stem cell transplantation.^{48,49} Plerixafor, in combination with Avastin (an anti-VEGF antibody) is now under intense investigation in a phase I clinical trial with the aim of preventing the growth of recurrent high-grade gliomas (NCT01339039⁵⁰).

Taken together, our observations reported in the present manuscript, as well as our previous work,³ have demonstrated that the SVZ environment is able to attract and harbor GSCs via the CXCL12/CXCR4 pathway. By this chemokine signaling system, it is therefore tempting to speculate if neurogenic zones in the adult brain may constitute a reservoir for tumor recurrence. Counteracting with the molecular mechanisms, which drive the migration of GSCs to neurogenic zones, might therefore be of great importance for future definition of therapeutic strategies.

Supplementary Material

Supplementary material is available at *Neuro-Oncology Journal* online (<http://neuro-oncology.oxfordjournals.org/>).

Funding

This work was supported by grants from the National Fund for Scientific Research (F.N.R.S/F.R.I.A); the Special Funds of the University of Liege; the Anti-Cancer Center near the University of Liège and the Leon Fredericq Foundation.

Acknowledgments

The authors are grateful to Dr. Pierre Robe (UMC) for the precious gift of resected glioblastoma cells established as primary cultures (GBM1 and GBM2). The authors also want to thank Dr. Claire Josse, the GIGA Viral Vector Platform, and the GIGA Imaging Platform for valuable technical support.

Conflict of interest statement. The authors declare that they have no conflicts of interest.

References

- Louis DN, Ohgaki H, Wiestler OD, et al. The 2007 WHO classification of tumours of the central nervous system. *Acta Neuropathol.* 2007;114(2):97–109.
- Furnari FB, Fenton T, Bachoo RM, et al. Malignant astrocytic glioma: genetics, biology, and paths to treatment. *Genes Dev.* 2007; 21(21):2683–2710.
- Kroonen J, Nassen J, Boulanger YG, et al. Human glioblastoma-initiating cells invade specifically the subventricular zones and olfactory bulbs of mice after striatal injection. *Int J Cancer.* 2011;129(3):574–585.
- Sadahiro H, Yoshikawa K, Ideguchi M, et al. Pathological features of highly invasive glioma stem cells in a mouse xenograft model. *Brain Tumor Pathol.* 2013;30(2):1–8.
- Scadden DT. The stem-cell niche as an entity of action. *Nature.* 2006;441(7097):1075–1079.
- Shen Q, Goderie SK, Jin L, et al. Endothelial cells stimulate self-renewal and expand neurogenesis of neural stem cells. *Science.* 2004;304(5675):1338–1340.
- Calabrese C, Poppleton H, Kocak M, et al. A perivascular niche for brain tumor stem cells. *Cancer Cell.* 2007;11(11):69–82.
- Folkins C, Man S, Xu P, et al. Anticancer therapies combining antiangiogenic and tumor cell cytotoxic effects reduce the tumor stem-like cell fraction in glioma xenograft tumors. *Cancer Res.* 2007;67(8):3560–3564.
- Rempel SA, Dudas S, Ge S, et al. Identification and localization of the cytokine SDF1 and its receptor, CXC chemokine receptor 4, to regions of necrosis and angiogenesis in human glioblastoma. *Clin Cancer Res.* 2000;6(1):102–111.
- Ehtesham M, Winston JA, Kabos P, et al. CXCR4 expression mediates glioma cell invasiveness. *Oncogene.* 2006;25(19): 2801–2806.
- Rubin JB, Kung AL, Klein RS, et al. A small-molecule antagonist of CXCR4 inhibits intracranial growth of primary brain tumors. *Proc Natl Acad Sci USA.* 2003;100(23):13513–13518.
- Bian XW, Yang SX, Chen JH, et al. Preferential expression of chemokine receptor CXCR4 by highly malignant human gliomas and its association with poor patient survival. *Neurosurgery.* 2007;61(3):570–578; discussion 578–579.
- Oh JW, Drabik K, Kutsch O, et al. CXC chemokine receptor 4 expression and function in human astroglia cells. *J Immunol.* 2001;166(4):2695–2704.
- Polajeva J, Sjosten AM, Lager N, et al. Mast cell accumulation in glioblastoma with a potential role for stem cell factor and chemokine CXCL12. *PLoS One.* 2011;6(9):e25222.
- Lee A, Kessler JD, Read TA, et al. Isolation of neural stem cells from the postnatal cerebellum. *Nat Neurosci.* 2005;8(6):723–729.
- Mirzadeh Z, Doetsch F, Sawamoto K, et al. The subventricular zone en-face: wholemount staining and ependymal flow. *J Vis Exp.* 2010;6(39):1938.
- Lin F, Baldessari F, Gyenge CC, et al. Lymphocyte electrotaxis in vitro and in vivo. *J Immunol.* 2008;181(4):2465–2471.
- Qiang L, Yang Y, Ma YJ, et al. Isolation and characterization of cancer stem like cells in human glioblastoma cell lines. *Cancer Lett.* 2009;279(1):13–21.
- do Carmo A, Patricio I, Cruz MT, et al. CXCL12/CXCR4 promotes motility and proliferation of glioma cells. *Cancer Biol Ther.* 2010; 9(1):56–65.
- Ehtesham M, Mapara KY, Stevenson CB, et al. CXCR4 mediates the proliferation of glioblastoma progenitor cells. *Cancer Lett.* 2009; 274(2):305–312.
- Lathia JD, Gallagher J, Heddleston JM, et al. Integrin alpha 6 regulates glioblastoma stem cells. *Cell Stem Cell.* 2010;6(5): 421–432.
- Burns JM, Summers BC, Wang Y, et al. A novel chemokine receptor for SDF-1 and I-TAC involved in cell survival, cell adhesion, and tumor development. *J Exp Med.* 2006;203(9):2201–2213.
- Hattermann K, Held-Feindt J, Lucius R, et al. The chemokine receptor CXCR7 is highly expressed in human glioma cells and mediates antiapoptotic effects. *Cancer Res.* 2010;70(8): 3299–3308.
- Sun X, Cheng G, Hao M, et al. CXCL12/CXCR4/CXCR7 chemokine axis and cancer progression. *Cancer Metastasis Rev.* 2010;29(4): 709–722.
- Hendrix CW, Flexner C, MacFarland RT, et al. Pharmacokinetics and safety of AMD-3100, a novel antagonist of the CXCR-4 chemokine receptor, in human volunteers. *Antimicrob Agents Chemother.* 2000;44:1667–1673.
- Gerlach LO, Skerlj RT, Bridger GJ, et al. Molecular interactions of cyclam and bicyclam non-peptide antagonists with the CXCR4 chemokine receptor. *J Biol Chem.* 2001;276(17):14153–14160.
- Vooijs M, Jonkers J, Lyons S, et al. Noninvasive imaging of spontaneous retinoblastoma pathway-dependent tumors in mice. *Cancer Res.* 2002;62(6):1862–1867.
- Liu G, Yuan X, Zeng Z, et al. Analysis of gene expression and chemoresistance of CD133+ cancer stem cells in glioblastoma. *Mol Cancer.* 2006;5(5):67.
- Lim YC, Roberts TL, Day BW, et al. A role for homologous recombination and abnormal cell-cycle progression in radioresistance of glioma-initiating cells. *Mol Cancer Ther.* 2012; 11(9):1863–1872.
- Trautmann F, Cojoc M, Kurth I, et al. CXCR4 as Biomarker for Radioresistant Cancer Stem Cells. *Int J Radiat Biol.* 2014; doi:10.3109/09553002.2014.906766.
- Lima FR, Kahn SA, Soletti RC, et al. Glioblastoma: therapeutic challenges, what lies ahead. *Biochim Biophys Acta.* 2012; 1826(2):338–349.
- Lathia JD, Heddleston JM, Venere M, et al. Deadly teamwork: neural cancer stem cells and the tumor microenvironment. *Cell Stem Cell.* 2011;8(5):482–485.
- Alvarez-Buylla A, Lim DA. For the long run: maintaining germinal niches in the adult brain. *Neuron.* 2004;41(5):683–686.
- Evers P, Lee PP, DeMarco J, et al. Irradiation of the potential cancer stem cell niches in the adult brain improves progression-free survival of patients with malignant glioma. *BMC Cancer.* 2010; 10:384.
- Eyler CE, Rich JN. Survival of the fittest: cancer stem cells in therapeutic resistance and angiogenesis. *J Clin Oncol.* 2008; 26(17):2839–2845.
- Bao S, Wu Q, McLendon RE, et al. Glioma stem cells promote radioresistance by preferential activation of the DNA damage response. *Nature.* 2006;444(7120):756–760.
- Jiang Y, Uhrbom L. On the origin of glioma. *Ups J Med Sci.* 2012; 117(2):113–121.
- Goffart N, Kroonen J, Rogister B. Glioblastoma-initiating cells: relationship with neural stem cells and the micro-environment. *Cancers (Basel).* 2013;5(3):1049–1071.

39. Lim DA, Cha S, Mayo MC, et al. Relationship of glioblastoma multiforme to neural stem cell regions predicts invasive and multifocal tumor phenotype. *Neuro Oncol.* 2007;9(4):424–429.
40. Zhang J, Sarkar S, Yong VW. The chemokine stromal cell derived factor-1 (CXCL12) promotes glioma invasiveness through MT2-matrix metalloproteinase. *Carcinogenesis.* 2005;26(12):2069–2077.
41. Gatti M, Pattarozzi A, Bajetto A, et al. Inhibition of CXCL12/CXCR4 autocrine/paracrine loop reduces viability of human glioblastoma stem-like cells affecting self-renewal activity. *Toxicology.* 2013;314(2–3):209–220.
42. Gilbertson RJ, Rich JN. Making a tumour's bed: glioblastoma stem cells and the vascular niche. *Nat Rev Cancer.* 2007;7(10):733–736.
43. Shen Q, Wang Y, Kokovay E, et al. Adult SVZ stem cells lie in a vascular niche: a quantitative analysis of niche cell-cell interactions. *Cell Stem Cell.* 2008;3(3):289–300.
44. Tavazoie M, Van der Veken L, Silva-Vargas V, et al. A specialized vascular niche for adult neural stem cells. *Cell Stem Cell.* 2008;3(3):279–288.
45. Galan-Moya EM, Le Guelte A, Lima Fernandes E, et al. Secreted factors from brain endothelial cells maintain glioblastoma stem-like cell expansion through the mTOR pathway. *EMBO Rep.* 2011;12(5):470–476.
46. Filipovic R, Zecevic N. The effect of CXCL1 on human fetal oligodendrocyte progenitor cells. *Glia.* 2008;56(1):1–15.
47. Liu C, Sage JC, Miller MR, et al. Mosaic analysis with double markers reveals tumor cell of origin in glioma. *Cell.* 2011;146(2):209–221.
48. Micallef IN, Stiff PJ, Stadtmauer EA, et al. Safety and efficacy of upfront plerixafor + G-CSF versus placebo + G-CSF for mobilization of CD34 hematopoietic progenitor cells in patients ≥ 60 and < 60 years of age with non-Hodgkin's lymphoma or multiple myeloma. *Am J Hematol.* 2013;88:1017–1023.
49. Dugan MJ, Maziarz RT, Bensinger WI, et al. Safety and preliminary efficacy of plerixafor (Mozobil) in combination with chemotherapy and G-CSF: an open-label, multicenter, exploratory trial in patients with multiple myeloma and non-Hodgkin's lymphoma undergoing stem cell mobilization. *Bone Marrow Transplant.* 2010;45(1):39–47.
50. Institute D-FC. Plerixafor (AMD3100) and Bevacizumab for Recurrent High-Grade Glioma. Available at: <http://clinicaltrials.gov/ct2/show/study/NCT01339039>. Accessed April 6, 2011.